SUPPORTING INFORMATION

Outstanding electrochemical performances of highly N- and O-doped carbons derived from pine tannin

Angela Sanchez-Sanchez [a,*], *Maria Teresa Izquierdo* [b], *Sandrine Mathieu* [c], *Julia González-Álvarez* [d], *Alain Celzard* [a], *Vanessa Fierro* [a,*]

[a] Institut Jean Lamour, UMR CNRS-Université de Lorraine n°7198, ENSTIB, 27 Rue Philippe Séguin, BP 21042, 88051 Epinal Cedex 9, France. *Corresponding authors: angela.sanchez-sanchez@univ-lorraine.fr; vanessa.fierro@univ-lorraine.fr

[b] Instituto de Carboquimica, ICB-CSIC, Miguel Luesma Castan, 4, 50018 Zaragoza, Spain

[c] Institut Jean Lamour, UMR CNRS-Université de Lorraine n°7198, Parc de Saurupt, CS 50840, 54011 Nancy Cedex, France.

[d] Department of Chemical Engineering, Universidade de Santiago de Compostela, 15782 Santiago de Compostela, Spain

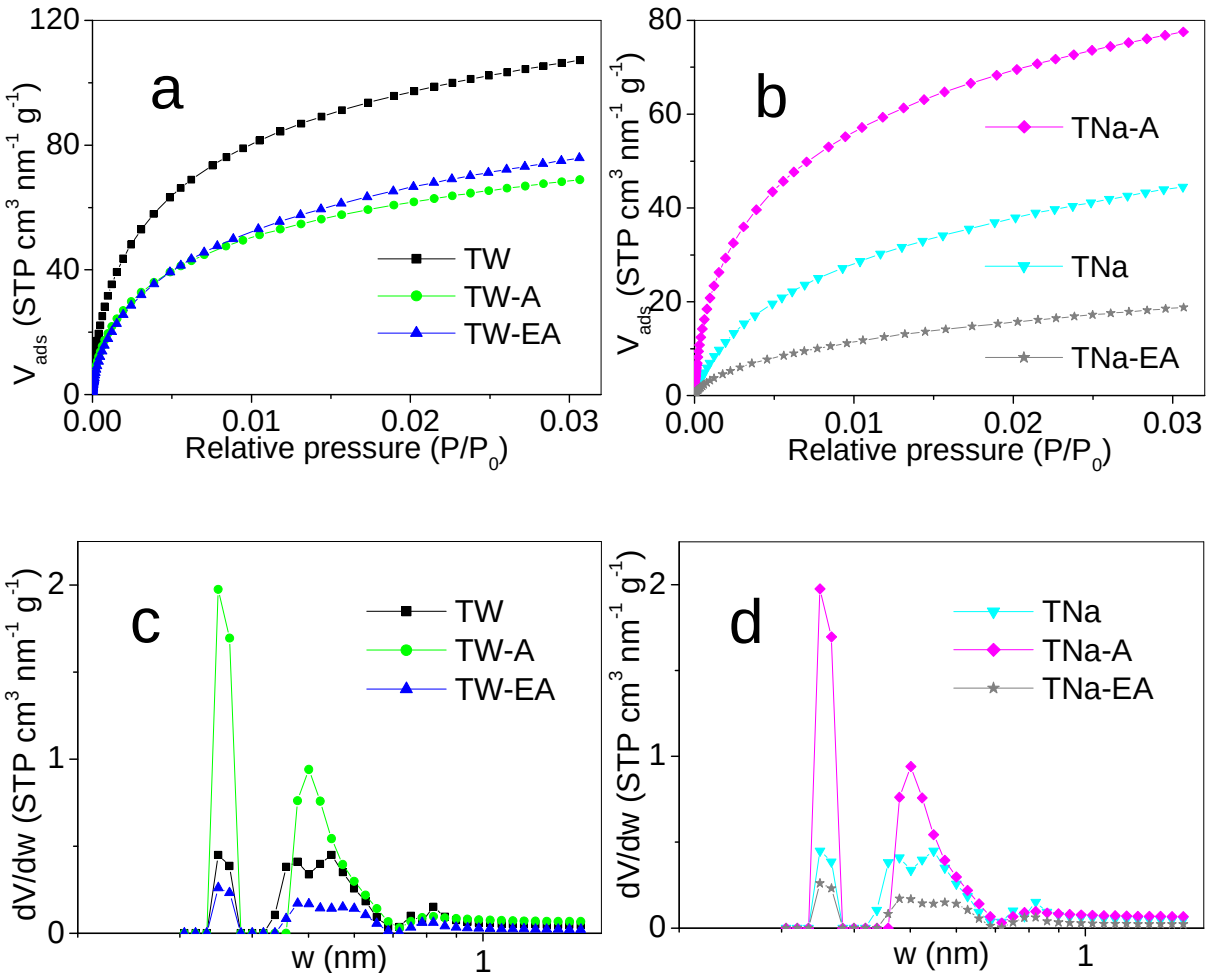

Figure S1. Carbon dioxide adsorption isotherms of the studied carbons (a and b) and PSDs calculated through the Non Local Density Functional Theory (NLDFT) applied to slit pores in equilibrium conditions (Quantachrome AS1Win software) (c and d).

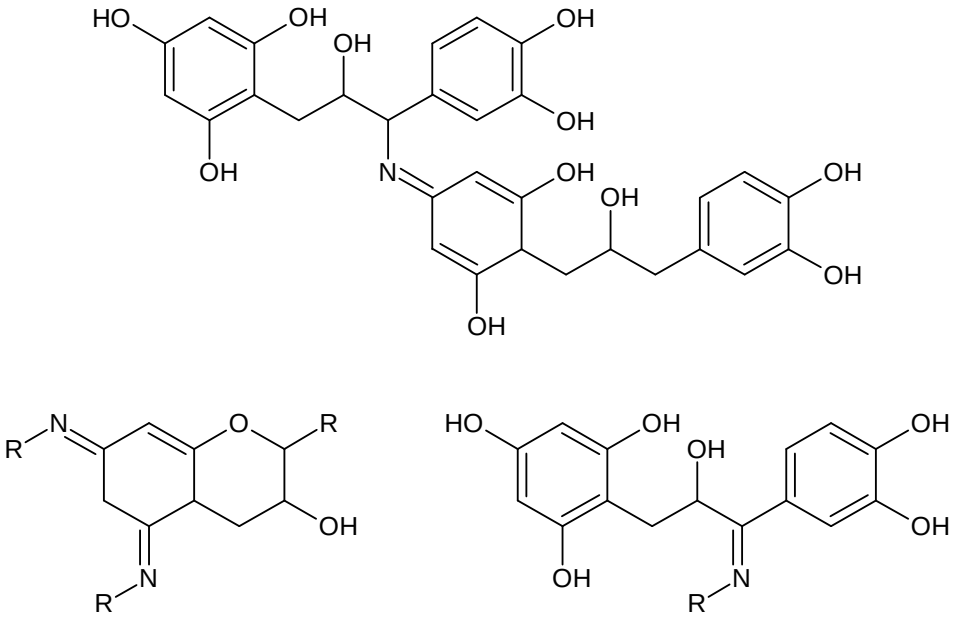

Figure S2. Some fragments and molecules identified in aminated hydrochars by CP-MAS ^{13}C NMR and MALDI-ToF spectroscopy. These molecules also contain abundant functional groups such as quinones, amines and amides.

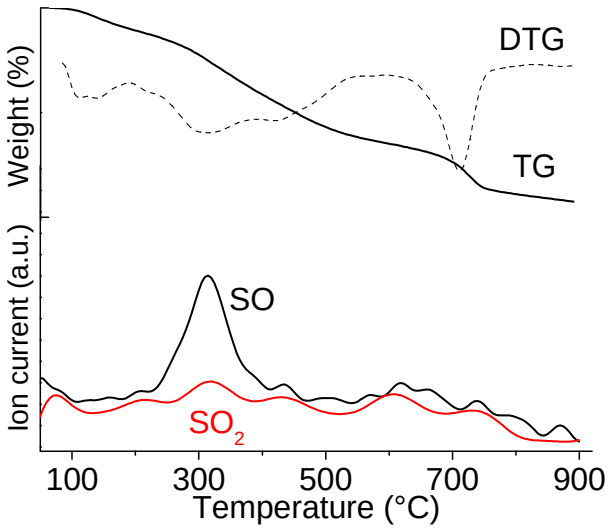

Figure S3. TG/DTG curves and evolution of SO and SO_2 gases released from TNa-EA hydrochar, determined by mass spectrometry (*m*/*z* values of 48 and 80, respectively).

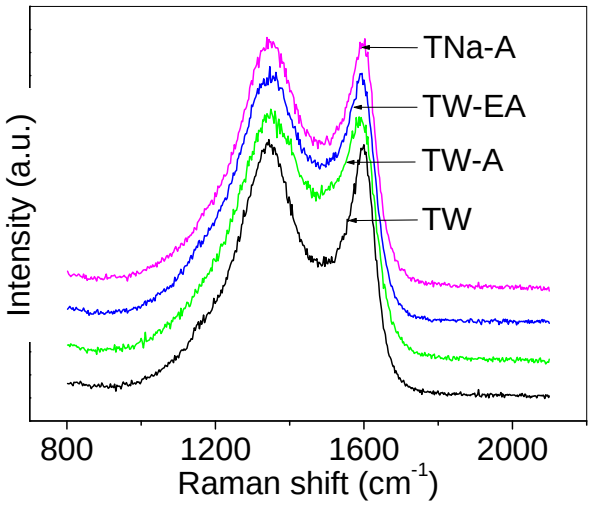

Figure S4. Raman spectra of representative carbon materials: TW, TW-A, TW-EA and TNa-A.

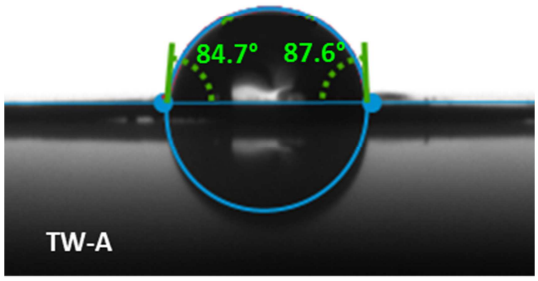

Figure S5. Contact angle of a representative electrode made from TW-A carbon.

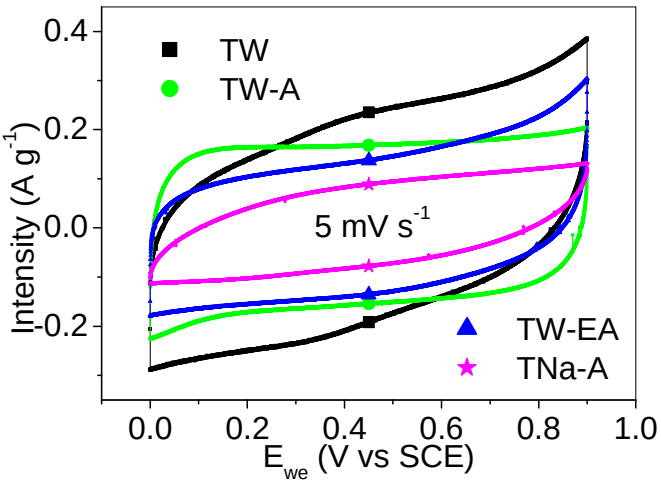

Figure S6. CV curves of the carbon electrodes at 5 mV s^{-1} scan rate obtained in a three–electrode cell with 1M H_2SO_4 electrolyte.

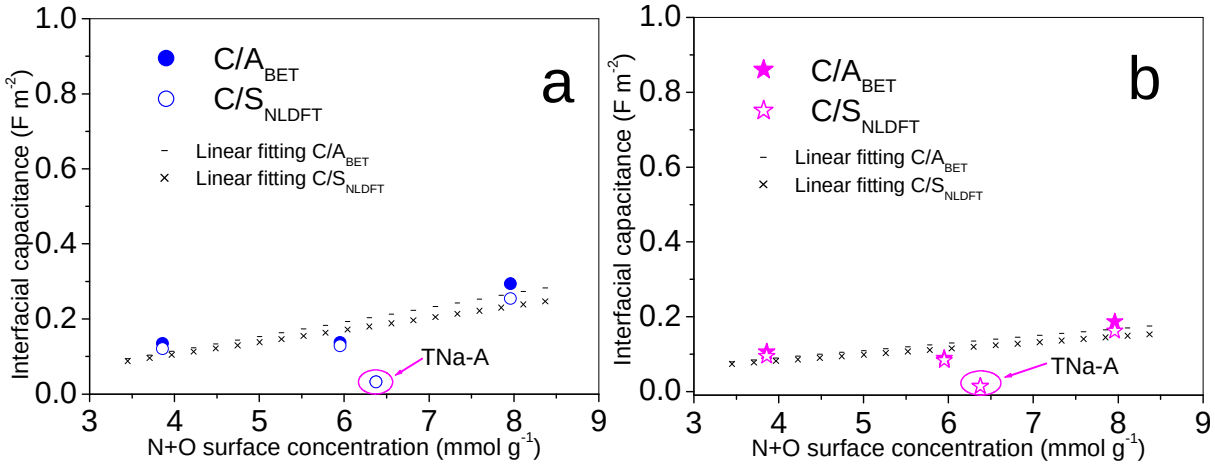

Figure S7. Plot of the interfacial capacitance versus the surface heteroatom concentration at: a) 100 mV s^{-1}; b) 1 V s^{-1}.

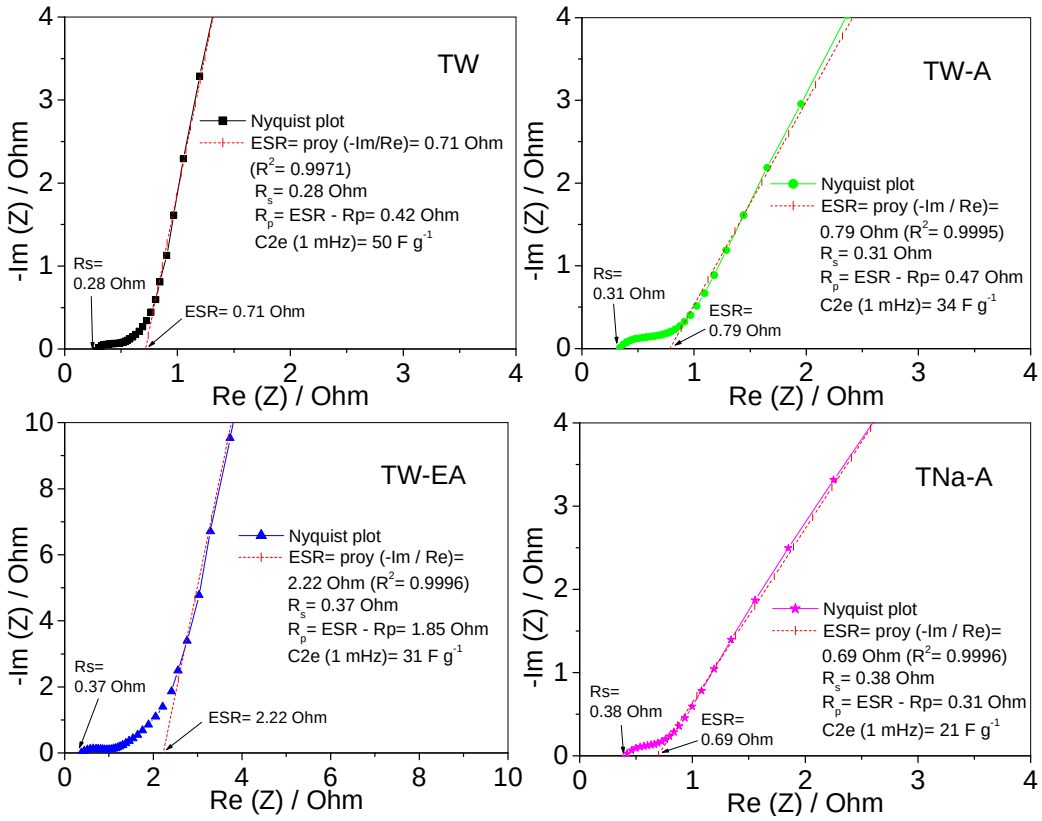

Figure S8. Nyquist plots and the corresponding fitting data of the studied carbons.

Table S1. Bulk chemical composition of the carbon materials determined by elemental analysis.

Sample	Elemental analysis (wt.%)				
	C	N	H	S	O
TW	92.0	0.7	0.7	0.1	6.5
TW-A	76.0	5.9	1.7	0.0	16.4
TW-EA	82.7	2.2	1.9	0.9	12.3
TNa	90.1	0.6	0.7	3.0	5.6
TNa-A	78.8	6.3	1.6	0.1	13.2
TNa-EA	81.0	2.4	0.8	3.5	12.3

Table S2. Data obtained from the first-order Raman spectra of the studied carbons.

Sample	D band		G band		I(D)/I(G) ratio
	Shift (cm^{-1})	Intensity (counts)	Shift (cm^{-1})	Intensity (counts)	
TW	1344.17	2822.64	1600.31	2771.39	1.0185
TW-A	1349.60	2403.96	1587.18	2336.66	1.0288
TW-EA	1346.89	3141.64	1595.06	3066.64	1.0244
TNa-A	1338.74	2893.04	1602.93	2880.35	1.0044

Table S3. Contributions to the C1s, O1s and N1s peaks.*

Sample	Surface Concentration (wt.%)			BE [eV] and relative peak areas [%] (in parentheses)											
				C1s peak					O1s peak			N1s peak			
	C	N	O	CI	CII	CIII	CIV	Shake-up satellite π–π	OI	OII	OIII	N6	N5	N-Q	N-X
TW	93.9	0.3	5.8	284.5 (65.1)	286.3 (25.4)	287.7 (5.7)	289.2 (0.7)	290.6 (3.1)	531.5 (33.4)	533.7 (64.4)	535.7 (2.2)	398.0 (14.8)	-	401.3 (85.2)	-
TW-A	87.9	4.5	7.5	284.4 (56.5)	285.5 (34.5)	287.7 (5.5)	289.2 (2.6)	290.6 (0.9)	531.2 (16.4)	532.5 (80.6)	534.7 (2.9)	398.1 (27.6)	400.3 (37.8)	401.1 (27.9)	402.6 (6.7)
TW-EA	90.7	1.4	8.0	284.5 (63.6)	285.5 (28.3)	287.7 (5.2)	289.4 (1.7)	290.5 (1.2)	531.2 (25.4)	532.7 (74.5)	-	398.3 (32.2)	400.5 (44.2)	401.2 (15.6)	402.3 (7.9)
TNa-A	90.4	4.3	5.2	284.4 (56.8)	285.6 (33.6)	287.7 (6.3)	289.2 (1.9)	290.4 (1.4)	530.9 (33.6)	532.5 (62.4)	534.6 (4.0)	398.0 (32.9)	400.3 (33.6)	401.0 (28.0)	402.6 (5.5)

*Assignments of the peaks: CI: hydrocarbons, aromatics, aliphatics; CII: Csp^3 and C-O bonds associated to ethers, phenols and anhydrides; CIII: C=O bond in carbonyls and quinones; CIV: C-O bonds in carboxyl acids; CV= plasmon loss or shake-up π–π satellite; OI: C=O bonds in quinone-type groups, carbonyls and carboxylic acids; OII: –OH bonds in phenols, C–O–C bonds in ethers and C=O bonds in ester and anhydride groups; OIII: chemisorbed oxygen, C-O bonds in esters and anhydrides, COOH carboxylic groups and/or water; N6: pyridinic nitrogen; N5: pyrrolic nitrogen; N-Q: quaternary nitrogen; N-X: nitrogen oxides.

Table S4. Electrochemical performance data of previously studied carbon materials (*Data not shown in publications).

Precursors	**A_{BET} (m^2 g^{-1})**	**Heteroatom concentration**	**Electrochemical measurements**	**Electrochemical performance: C (F g^{-1}); E (W h Kg^{-1}); P (W Kg^{-1})**	**Ref.**
Sugarcane molasses, direct carbonisation	8	18.3 at.% O (surface) 2.7 at.% S (surface)	*Cyclic voltammetry:* Three-electrode 1M H_2SO_4 *Galvanostatic charge-discharge:* Two-electrode 1M H_2SO_4	153 F g^{-1} (CV, 0.5 mV s^{-1}); 6.9 W h kg^{-1}; 132 W kg^{-1} (GCD, 0.1 A g^{-1})	37
Corncobs / KOH activation Norit A Supra (commercial activated carbon)	3054 1899	9.49 at.% O < 0.3 at.% N 9.64 at.% O < 0.3 at.% N	Three-electrode 0.5M H_2SO_4	401.6 F g^{-1} (0.5 A g^{-1}) 160 F g^{-1} (0.5 A g^{-1})	57
Bamboo / KOH activation / Boron doping / Nitrogen doping	172	Atomic ratios: B/C= 1.32% N/C= 0.95%	Three-electrode 1M H_2SO_4	318 F g^{-1} (0.2 A g^{-1}); 42.1 Wh kg^{-1}; 95 W kg^{-1}	61
Coconut shells / H_2O_2 and $ZnCl_2$ pre-treatments / CO_2 activation	2440	*	Three-electrode 1M H_2SO_4	246 F g^{-1} (0.25 A g^{-1}); 7.6 Wh kg^{-1}; 4.5 W kg^{-1}	62
Ethylenediamine, carbon tetrachloride / KOH activation	1913	5.54 at.% O 1.10 at.% N	Three-electrode 1M H_2SO_4	303 F g^{-1} (0.1 A g^{-1})	65
Cocoons of Bombyx mori / KOH activation	3841	*	Three-electrode 6M KOH	408 F g^{-1} (0.5 A g^{-1}); 17.4 Wh kg^{-1}; 1002 W kg^{-1}	67
Commercial activated carbon (Maxsorb)	3310	*	Three-electrode 30 wt.% KOH	333.9 F g^{-1} (5 mV s^{-1}); 9.4-2.1 Wh kg^{-1}; 190-410 W kg^{-1}	69